Proceedings of the 3rd International Congress APMAS2013, April 24–28, 2013, Antalya, Turkey

Coating Effect on Magnetic Properties of $Fe_{36}Co_{36}B_{19.2}Si_{4.8}Mo_3W_1$ Amorphous Ribbons

F. Perincek, M. Haciismailoglu, K. Sarlar, M.C. Haciismailoglu, M. Alper and I. Kucuk

Physics Department, Faculty of Arts and Sciences, Uludag University, Gorukle Campus, 16059 Bursa, Turkey

In this research, the electrodeposition technique was employed to prepare fine-grained nickel, iron and iron-cobalt coatings with 1 μm thicknesses on the substrate of the $Fe_{36}Co_{36}B_{19.2}Si_{4.8}Mo_3W_1$ amorphous ribbons. The coating effect on magnetic properties was examined at room temperature using an ADE Magnetics EV9 vibrating sample magnetometer with maximum magnetic field strength of 1750 kA/m. It is found that Ni, Fe, and Fe–Co coated amorphous ribbons show 0.60, 0.71, and 1.01 T saturation magnetization, respectively, while uncoated ribbon has 1.55 T.

DOI: 10.12693/APhysPolA.125.408

PACS: 81.05.Kf, 81.15.Pq, 81.15.−z, 75.70.Ak

1. Introduction

Since the first discovery of the ferromagnetic Fe-based metallic glasses in 1995, much effort has been devoted to the development of ferromagnetic bulk metallic glasses (BMGs) for both fundamental research and industrial applications [1]. Nowadays usually magnetic metallic glasses are produced in the shape of films, ribbons and wires with a small size in a least one dimension [1, 2]. Among them, ribbons and films are frequently used for microelectronics and sensor applications [3, 4]. The knowledge and the control of the bulk magnetic properties of magnetic metallic alloys are important in order to obtain miniaturized magnetic devices with improved performances [4].

Recently, studies are carried out on the coating of metallic glasses. The reason of it, the metallic glasses are promising candidates for industrial and technological applications due to their excellent physical (large elastic limit, high strength, high corrosion and wear resistance, etc.) and magnetic (high saturation magnetization, almost zero coercivity, etc.) properties [5–7]. There are different physical and chemical methods such as pulsed laser, sputtering, thermal evaporation, thermionic vacuum arc, chemical vapor deposition, anodization, etc. to prepare thin films [4]. Another method to produce thin films is electrodeposition. The electrodeposition method has advantages such as rapid production, low cost and easy control of deposition parameters [8, 9].

In this study we investigate the bulk magnetic behavior of the $Fe_{36}Co_{36}B_{19.2}Si_{4.8}Mo_3W_1$ amorphous ribbons produced by melt spinning uncoated and coated nickel, iron, and iron–cobalt that were produced by electrodeposition method. The effect of coating on the saturation magnetization and coercivity was also analyzed.

2. Experimental

The Fe–Co-based ingots with nominal compositions were first homogenized by arc melting the pure elements in Zr-gettered argon atmosphere for at least four times. Rapidly solidified $Fe_{36}Co_{36}B_{19.2}Si_{4.8}Mo_3W_1$ ribbon then was prepared by the single roller melt-spinning technique. During rapid cooling, a stream of molten alloy with temperature 1423 K was ejected by pressured argon from 0.5 mm diameter orifice onto brass wheel rotating at 30 m/s circumferential velocity. Resulting ribbon was typically 3 m long, 0.5 cm wide, and 25 μm thick.

The glass transition T_g, crystallization T_x, liquidus T_l and melting temperatures T_m were measured with Setaram SET-SYS 16/18 differential scanning calorimetry (DSC) under flowing high purity argon gas with 15–20 mg samples at a ramp rate of 0.67 K/s. X-ray diffraction (XRD) was conducted with Rigaku D/MAX 2200 by monochromatic Cu K_α radiation to evaluate whether the analyzed region of the specimen is amorphous or retains crystalline phases.

Ni, Fe, and Fe–Co alloy films were electrodeposited on $Fe_{36}Co_{36}B_{19.2}Si_{4.8}Mo_3W_1$ amorphous ribbon substrates using a potentiostat/galvanostat with three electrodes. Ni films were prepared from an electrolyte consisting of 2.0 M nickel sulfamate and 0.5 M boric acid. In the case of the Fe films, an electrolyte consisting of 1 M iron sulphate and 0.5 M boric acid was used. And finally, for depositing the Fe–Co films, the electrolyte was 0.5 M cobalt sulphate, 0.1 M iron sulphate, and 0.3 M boric acid. All chemicals were reagent grade and dissolved in distilled water and are listed in Table I. A platinum (Pt) sheet was used as counter electrode. The reference electrode was a saturated calomel electrode (SCE). $Fe_{36}Co_{36}B_{19.2}Si_{4.8}Mo_3W_1$ amorphous ribbon with an area of 0.49 cm^2 was served as a substrate. Prior to deposition, the substrate was washed in distilled water. The nominal thickness of all films was fixed at 1 μm according to the Faraday law.

The bulk magnetic properties of coated and uncoated amorphous ribbons were examined at room temperature using an ADE Magnetics EV9 vibrating sample magnetometer (VSM) with maximum magnetic field strength

TABLE I

Electrolytes prepared for the present work.

Status of coating	Nickel sulfamate Ni $(SO_3NH_2)_2 \cdot 4H_2O$ [M]	Cobalt sulfate $CoSO_4 \cdot 7H_2O$ [M]	Iron sulphate $FeSO_4 \cdot 7H_2O$ [M]	Boric acid H_3BO_3 [M]
Ni coated	2.0	–	–	0.5
Fe coated	–	–	1.0	0.5
Fe–Co coated	–	0.5	0.1	0.3

of 1750 kA/m, real-time field control and dynamic Gauss range capable of reaching a resolution of 0.08 A/m at low fields.

3. Results and discussion

Figure 1a shows that the DSC pattern obtained for rapidly solidified $Fe_{36}Co_{36}B_{19.2}Si_{4.8}Mo_3W_1$ ribbon undergoes glass transition at 787 K which is followed by a subsequent crystallization at 831 K. Thereby, supercooled liquid region ($\Delta T_x = T_x - T_g$) of 44 K is obtained for the $Fe_{36}Co_{36}B_{19.2}Si_{4.8}Mo_3W_1$ amorphous ribbon. On the other hand, temperature of melting (T_m) and liquidus temperature (T_l) are shown in Fig. 1b, 1350 K and 1428 K, respectively. Thus, the reduced glass transition temperature ($T_{rg} = T_g/T_l$) of 0.55 is calculated.

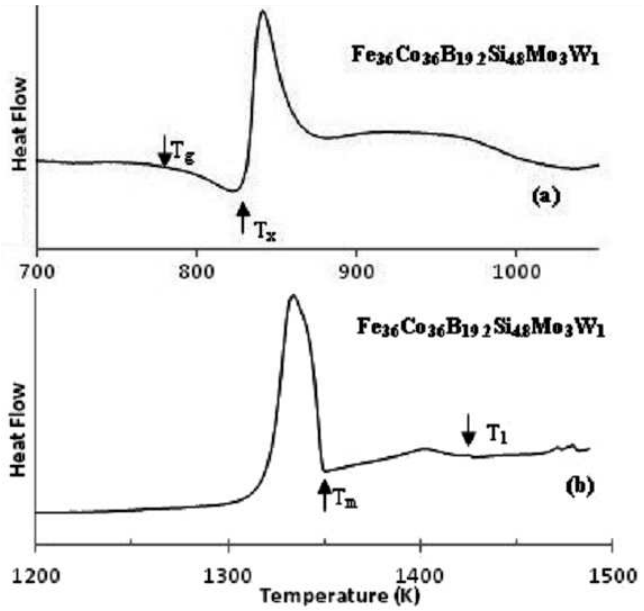

Fig. 1. DSC patterns of $Fe_{36}Co_{36}B_{19.2}Si_{4.8}Mo_3W_1$ melt spun ribbon: (a) T_g and T_x, (b) T_m and T_l.

The XRD pattern of $Fe_{36}Co_{36}B_{19.2}Si_{4.8}Mo_3W_1$ ribbon is shown in Fig. 2. It can be depicted from XRD pattern of ribbon that the $Fe_{36}Co_{36}B_{19.2}Si_{4.8}Mo_3W_1$ alloy is fully amorphous, as evidenced by the absence of diffraction peaks.

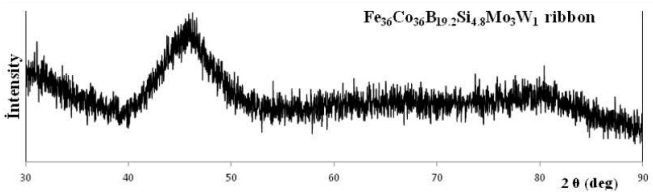

Fig. 2. Characteristic XRD pattern of $Fe_{36}Co_{36}B_{19.2}Si_{4.8}Mo_3W_1$ melt spun ribbon.

The hysteresis loops for the $Fe_{36}Co_{36}B_{19.2}Si_{4.8}Mo_3W_1$ amorphous ribbons produced by melt spinning uncoated and coated nickel, iron, and iron–cobalt produced by electrodeposition method are shown in Fig. 3. The saturation magnetization and coercivity values of uncoated, coated nickel, iron, and iron–cobalt $Fe_{36}Co_{36}B_{19.2}Si_{4.8}Mo_3W_1$ amorphous ribbons are also listed in Table II.

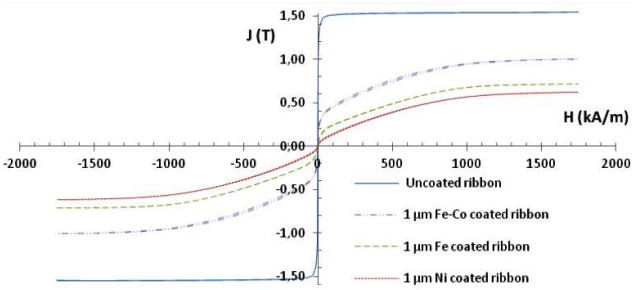

Fig. 3. The bulk hysteresis loop of the $Fe_{36}Co_{36}B_{19.2}Si_{4.8}Mo_3W_1$ amorphous ribbons produced by melt spinning uncoated and coated nickel, iron, and iron–cobalt produced by electrodeposition method.

TABLE II

A comparison of the saturation magnetization and coercivity values of $Fe_{36}Co_{36}B_{19.2}Si_{4.8}Mo_3W_1$ amorphous ribbon.

Status of coating	Saturation magnetization [T]	Coercivity [A/m]
uncoated ribbon	1.55	11.2
1 μm Fe–Co coated ribbon	1.01	54.7
1 μm Fe coated ribbon	0.71	138.9
1 μm Ni coated ribbon	0.60	256.7

As seen from Table II, the saturation magnetization values decrease when amorphous ribbons are coated with Ni, Fe, and Fe–Co. The decrease in the saturation magnetization and increase in the coercivity of coated ribbons can be explained as the consequences of the competing ferromagnetic and antiferromagnetic exchange interactions of the interstitial atoms with the rest of the $Fe_{36}Co_{36}B_{19.2}Si_{4.8}Mo_3W_1$ amorphous ribbon [10].

4. Conclusion

Amorphous magnetic $Fe_{36}Co_{36}B_{19.2}Si_{4.8}Mo_3W_1$ ribbons have been fabricated by the single roller melt-spinning technique. Then, these ribbons have been successfully coated with Ni, Fe, and Fe–Co by the electrodeposition method. It is seen that Ni, Fe, and Fe–Co coated amorphous ribbons show less saturation magnetization and higher coercivity when compared to their uncoated ones. Coating has produced a significant change in the magnetic properties of the ribbons including the decrease in saturation magnetization and increase in coercivity.

Acknowledgments

This work was supported by the Commission of Scientific Research Projects of Uludag University, project numbers UAP(F)-2012/27 and HDP(F)-2012/39.

References

[1] I. Kucuk, M. Aykol, O. Uzun, M. Yildirim, M. Kabaer, N. Duman, F. Yilmaz, K. Erturk, M.V. Akdeniz, A.O. Mekhrabov, *J. Alloy Comp.* **509**, 2334 (2011).

[2] F. Li, T. Zhang, A. Inoue, S. Guan, N. Shen, *Intermetallics* **12**, 1139 (2004).

[3] M. Neagu, M. Dobromir, G. Popa, H. Chiriac, G. Singurel, C. Hison, *Sens. Actuat. A* **129**, 172 (2006).

[4] F. Perincek, K. Erturk, M. Aykol, I. Kucuk, M.V. Akdeniz, *Acta Phys. Pol. A* **121**, 147 (2012).

[5] W. Chen, K.C. Chana, P. Yu, G. Wang, *Mater. Sci. Eng. A* **528**, 2988 (2011).

[6] C. Zhang, R.Q. Guo, Y. Yang, Y. Wu, L. Liu, *Electrochim. Acta* **56**, 6380 (2011).

[7] F.X. Qin, X.M. Wang, G.Q. Xie, K. Wada, M. Song, K. Furuya, K. Asami, A. Inoue, *Intermetallics* **17**, 945 (2009).

[8] M. Haciismailoglu, M. Alper, *Surf. Coat. Technol.* **206**, 1430 (2011).

[9] M. Safak, M. Alper, H. Kockar, *J. Magn. Magn. Mater.* **304**, e784 (2006).

[10] P. Kharel, X.Z. Li, V.R. Shah, N.A. Aqtash, K. Tarawneh, R.F. Sabirianov, R. Skomski, D.J. Sellmyer, *J. Appl. Phys.* **111**, 07E326 (2012).